Emergent Elasticity in Amorphous Solids

Jishnu N. Nampoothiri,[1,2] Yinqiao Wang,[3] Kabir Ramola,[2] Jie Zhang,[3]
Subhro Bhattacharjee,[4] and Bulbul Chakraborty[1]

[1]*Martin Fisher School of Physics, Brandeis University, Waltham, Massachusetts 02454, USA*
[2]*Centre for Interdisciplinary Sciences, Tata Institute of Fundamental Research, Hyderabad 500107, India*
[3]*Institute of Natural Sciences and School of Physics and Astronomy, Shanghai Jiao Tong University, Shanghai 200240 China*
[4]*International Centre for Theoretical Sciences, Tata Institute of Fundamental Research, Bengaluru 560089, India*

(Received 17 April 2020; revised 14 July 2020; accepted 11 August 2020; published 10 September 2020)

The mechanical response of naturally abundant amorphous solids such as gels, jammed grains, and biological tissues are not described by the conventional paradigm of broken symmetry that defines crystalline elasticity. In contrast, the response of such athermal solids are governed by local conditions of mechanical equilibrium, i.e., force and torque balance of its constituents. Here we show that these constraints have the mathematical structure of a generalized electromagnetism, where the electrostatic limit successfully captures the anisotropic elasticity of amorphous solids. The emergence of elasticity from local mechanical constraints offers a new paradigm for systems with no broken symmetry, analogous to emergent gauge theories of quantum spin liquids. Specifically, our $U(1)$ rank-2 symmetric tensor gauge theory of elasticity translates to the electromagnetism of fractonic phases of matter with the stress mapped to electric displacement and forces to vector charges. We corroborate our theoretical results with numerical simulations of soft frictionless disks in both two and three dimensions, and experiments on frictional disks in two dimensions. We also present experimental evidence indicating that force chains in granular media are subdimensional excitations of amorphous elasticity similar to fractons.

DOI: 10.1103/PhysRevLett.125.118002

Introduction.—Solids that emerge in strongly nonequilibrium processes such as jamming [1–4] or gelation [5,6], are characterized by strong stress heterogeneities, often referred to as force chains. They are rigid in that they can sustain external shear, yet they are often fragile [2,3]. Analogous to classical elasticity theory [7], it is plausible to ask whether a long wavelength field theoretic description exists for the mechanical response of such athermal solids and if so, what are its characteristics and universal features, and what would be the appropriate variables that can account for the underlying kinetic constraints in the emergent field theory? Any attempt to construct such a field theory must answer (a) how to obtain the stress field, and (b) how to incorporate microscopic information about the structural disorder, accounting for the mechanical constraints into a continuum formulation. This second problem, in particular, has a close resemblance with kinetically constrained models such as hard-core dimer models on lattices where the hard-core constraint of each site being part of one and only one dimer naturally allows for an emergent gauge theory description at low energy and long wavelengths [8–10].

In this Letter, we develop a theory of stress transmission in disordered granular solids, both with and without friction, where the local constraints of mechanical equilibrium are paramount, i.e., every grain satisfies the constraints of force and torque balance. These local constraints imply that the grain-level stress tensor $\hat{\sigma}_g$ is symmetric [11,12] and satisfies

$$(\nabla \cdot \hat{\sigma})_g = \sum_{c \in g} \mathbf{f}_{g,c} = \mathbf{f}_g^{\text{ext}}. \tag{1}$$

Here, ∇ is a discrete divergence operator defined over the underlying contact network, as detailed in the Supplemental Material [13], $\mathbf{f}_{g,c}$ are the contact forces acting on grain g at contact c and $\mathbf{f}_g^{\text{ext}}$ is the total external force acting on the grain. Upon coarse-graining [24], Eq. (1) gives rise to the continuum condition of mechanical equilibrium:

$$\partial_i \sigma_{ij}(\mathbf{r}) = f_j(\mathbf{r}), \tag{2}$$

where $\sigma_{ij}(\mathbf{r})$ and $f_j(\mathbf{r})$ are the stress and external force density at the point $\mathbf{r}$, respectively.

Stress equation and tensorial electromagnetism.—Eq. (2), along with the symmetry of the stress tensor encapsulates the local constraints of mechanical equilibrium. Further, Eq. (2) can be casted as the exact analog of Gauss's law,

$$\partial_i E_{ij} = \rho_j, \tag{3}$$

in a generalized electromagnetism of $U(1)$ symmetric rank-2 tensor electric fields $E_{ij} = E_{ji}$ and vector charges

ρ_i with $i = 1, \ldots, d$ in d spatial dimensions, the so-called vector charge theory (VCT) of electromagnetism. The resultant generalized Maxwell equations automatically conserve the total charge ($\int d\mathbf{r}\boldsymbol{\rho} = 0$) and the dipole moment [$\int d\mathbf{r}(\mathbf{r} \times \boldsymbol{\rho}) = 0$] [25,26].

The correspondence between Eqs. (2) and (3), along with the conserved quantities makes VCT a natural starting point for deriving the correct continuum theory of the mechanical response of granular solids by formally mapping $E_{ij} \overset{?}{\leftrightarrow} \sigma_{ij}$ and vector charges to unbalanced forces, i.e., $\boldsymbol{\rho} \overset{?}{\leftrightarrow} \boldsymbol{f}$. This approach is similar to the problem of frustrated magnets and/or dimer models, where due to nontrivial local energetic or kinetic constraints, the individual spins or dimers cease to be the right degrees of freedom and hence fail to describe the low energy theory, which in turn is often described by emergent gauge fields that naturally capture the constraints [8–10,27]. Similarly, the displacement of the individual grains from the reference crystalline positions—the mainstay of the theory of elasticity of crystalline solids [28]—cease to be the right variables in the absence of broken translation symmetry. However, the long-range stress correlations generated by Newton's laws of force and torque balance are described correctly by the emergent electromagnetism.

As an immediate consequence of this mapping, we note that the two conservation laws lead to subdimensional propagation of charges—a feature of recently discussed fractonic phases of matter [25] as well as topological defects in elastic solids [29]. In the present context, it also provides a natural explanation for the visually striking "force chains" (see Fig. 3) observed in photoelastic images of granular solids [30], as our analysis will demonstrate.

It is well known [31] that Eq. (2) does not provide enough equations to solve for the field σ_{ij}, since there are only d equations for the $d(d+1)/2$ components of a symmetric tensor in d dimensions [25]. These missing equations are provided within VCT, by invoking the complete set of Maxwell's equations required to uniquely specify E_{ij}. In particular, the generalized Faraday's law: $(\partial B_{ij}/\partial t) = -\epsilon_{iab}\epsilon_{jcd}\partial_a\partial_c E_{bd}$, where $B_{ij} = B_{ji}$ is the tensor magnetic field of VCT, leads to the generalized irrotational condition $\epsilon_{iab}\epsilon_{jcd}\partial_a\partial_c E_{bd} = 0$ in the electrostatic limit. This condition provides the missing equations, and leads to the potential formulation: $E_{ij} = \frac{1}{2}(\partial_i\phi_j + \partial_j\phi_i)$, where ϕ_i is the electrostatic potential which can be used to obtain E_{ij} for *any* charge configuration [25].

Granular solid as a generalized dielectric medium.—The above gauge theory formulation containing all the basic ingredients, requires an extension—akin to that of dielectric media—to capture the complexity of the granular mechanics. This is easily seen by noting the twin crucial characteristics of granular media: (i) it is *only* defined under external pressure (as a packing of grains with purely repulsive interactions will fall apart in the absence of boundary forces), and (ii) it can support internal stresses. This translates, within VCT, to an assembly being subject to well defined boundary charges developing internal *charge dipoles*, akin to the response of a polarizable medium (dielectric). Alternatively stated, although a granular solid under external compression is free of "charges" since every grain satisfies force and torque balance, "bound charges" exist as pairs of equal and opposite forces at every contact of the disordered granular network. Hence, we rewrite Eq. (3) as

$$\partial_i E_{ij} = \rho_j^{\text{free}} + \rho_j^{\text{bound}}, \tag{4}$$

where ρ_j^{free} arises from any body-force such as gravity and ρ_j^{bound} are the bound charges arising from the force dipoles and can be accounted for using a tensorial dipole moment P_{ij} such that

$$\partial_i P_{ij} = -\rho_j^{\text{bound}}. \tag{5}$$

A complete derivation of these relations, and a detailed discussion of the structure of the theory will be presented in a future paper. The structure of P_{ij} is influenced by various microscopic details of the system such as the features of the underlying contact network and the nature of contact forces which, for example, can be purely repulsive or both repulsive and attractive and frictionless or frictional.

To construct a continuum theory, we assert that P_{ij} is related to E_{ij} through a fourth-rank polarizability tensor, χ_{ijkl}, as in linear dielectrics: $P_{ij} = \chi_{ijkl}E_{kl}$. Straightforward generalization of electrostatics in dielectric medium follows. We define a "displacement" tensor,

$$D_{ij} = (\delta_{ik}\delta_{jl} + \chi_{ijkl})E_{kl} = (\Lambda^{-1})_{ijkl}E_{kl}, \tag{6}$$

which satisfies

$$\partial_i D_{ij} = \rho_j^{\text{free}}; \qquad \epsilon_{iab}\epsilon_{jcd}\partial_a\partial_c(\Lambda D)_{bd} = 0. \tag{7}$$

The inverse dielectric tensor Λ satisfies $\Lambda_{ijkl} = \Lambda_{jikl} = \Lambda_{ijlk} = \Lambda_{jilk}$. Since the inherent stresses in a granular solid satisfy the first relation in Eq. (7) as a direct consequence of force balance, we interpret D_{ij} as the Cauchy stress tensor measured from contact forces and contact vectors inside the material, i.e., $D_{ij} \leftrightarrow \sigma_{ij}$ in Eq. (7).

Equation (7), which is our main theoretical result, can be compared to anisotropic elasticity [32]:

$$\partial_i\sigma_{ij} = 0; \qquad \epsilon_{iab}\epsilon_{jcd}\partial_a\partial_c U_{bd} = 0,$$
$$\sigma_{ij} = (\Xi)^{-1}_{ijkl}U_{kl}. \tag{8}$$

where U_{ij} is the macroscopic strain tensor. In Eq. (8), $\hat{\Xi}[\leftrightarrow \Lambda$ appearing in Eq.(7)] is the inverse of the elastic modulus tensor. Identifying $E_{ij} \leftrightarrow U_{ij}$, and $D_{ij} \leftrightarrow \sigma_{ij}$, demonstrates that an elasticity theory capturing the stress

responses in granular solids [32–34] emerges from VCT. A gauge potential, $\boldsymbol{\phi}$ replaces the displacement field in elasticity theory. We would like to reiterate that unlike the displacement field in elasticity, the gauge potential $\boldsymbol{\phi}$ is not a physical observable. Therefore, VCT provides the "missing" compatibility equations that allow us to solve the granular stress response problem without invoking a displacement field. Thus, although $\hat{D}$ and $\hat{E}$ have a correspondence with $\hat{\sigma}$ and $\hat{U}$, the elasticity emerges from local constraints and not from broken symmetry. This *stress-only* description does not refer to a stress-free state or displacement fields. Moreover, the effective elastic modulus $\hat{\Lambda}$ is not constrained by symmetries imposed by a free-energy and will depend on protocols.

We note that the missing equation in two dimensions had been obtained for the *particular* contact geometry of hard-particle frictional jammed states [24] by introducing a geometry-related symmetric tensor. The relation of this network-specific description to VCT needs to be explored further. However, the potential formulation [24] is identical to the dual representation of VCT in two dimensions [13,35].

Experiments and numerical results.—We have compared the predictions for stress-stress correlations obtained from Eq. (7) to experimental and numerical data, and extracted $\hat{\Lambda}$ for frictionless and frictional granular solids prepared under different protocols. A hallmark of the VCT in free space [Eq. (3)], both in two and three dimensions, is the appearance of pinch point singularities in the Fourier transforms of E_{ij} correlators [36]:

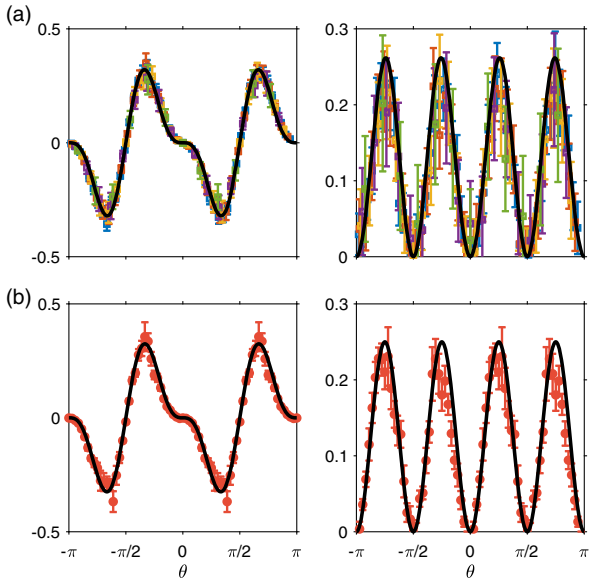

FIG. 1. Comparisons in Fourier space between the theoretical predictions (solid black line) and the disorder-averaged angular dependent stress-stress correlations $C_{xxxy}(\theta)$ and $C_{xxyy}(\theta)$ in the numerical: (a) and the experimental results (red symbols): (b), for isotropically jammed systems. The range of pressure for the numerical data is $P \in [0.016, 0.017]$ and the results are displayed for five different system sizes $N = 512$, 1024, 2048, 4096, 8192. The experimental data is from frictional packings with a range of pressure $P \in [1.5 \times 10^{-4}, 2.9 \times 10^{-4}]$. All correlation functions are normalized by the peak value of $C_{xxxx}(\theta)$. Here, $C_{ijkl} \equiv \langle \sigma_{ij}\sigma_{kl} \rangle$.

$$C^{\text{free}}_{ijkl}(\mathbf{q}) \equiv \langle E_{ij}(\mathbf{q})E_{kl}(-\mathbf{q})\rangle \propto \frac{(\delta_{ik}\delta_{jl}+\delta_{il}\delta_{jk})}{2} + \frac{q_i q_j q_k q_l}{q^4} - \frac{1}{2}\left(\frac{\delta_{ik}q_j q_l}{q^2} + \frac{\delta_{jk}q_i q_l}{q^2} + \frac{\delta_{il}q_j q_k}{q^2} + \frac{\delta_{jl}q_i q_k}{q^2}\right). \tag{9}$$

Equation (9) is obtained by imposing the Gauss's law constraint, $\partial_i E_{ij} = 0$, on Eq. (3), and assuming that all states are equiprobable [36], i.e., the Edwards measure [11]. Earlier granular field theories [37–39] based on this measure used a dual formulation of VCT [24,35] where the emergence of elasticity is not evident. Since $C^{\text{free}}_{ijkl}(\mathbf{q})$ is independent of $|\mathbf{q}|$, it is straightforward to show that the correlations in real space decay as $1/r^d$. A more stringent test of the theory, therefore is the pinch-point structure of the correlation functions.

For granular solids, we computed the correlators $C_{ijkl}(\mathbf{q}) = \langle D_{ij}(\mathbf{q})D_{kl}(-\mathbf{q})\rangle$ using Eq. (7), and tested the predictions in ensembles of 2D and 3D isotropically compressed soft particles (numerically), and in ensembles of 2D packings of frictional grains (experimentally). Pinch point singularities are clearly exhibited in both two dimensions (Figs. 1 and 3) and three dimensions (Fig. 2). We have determined $\hat{\Lambda}$ through detailed comparisons between theory and measurements of C_{ijkl} (Figs. 1–3). Figure 1 demonstrates that for packings created under isotropic compression, $\hat{\Lambda} = \lambda \mathbb{1}$, with $\mathbb{1}$ being the identity tensor. Additional tests of the theory are presented in the Supplemental Material [13].

To illustrate the sensitivity of the $\hat{\Lambda}$ tensor to protocol (stress ensemble) we generated sheared packings of the same grains used in the isotropic compression. Under the experimental conditions of pure shear, with principle stress along x and y, a diagonal form with different values of λ_{ii} provides an excellent description of the experimental observations (Fig. 3). We find that λ_{ii}, satisfy a set of bounds imposed by the constraint of positivity of normal forces in granular media [37,39].

A consequence of the pinch point singularities is that in real space, $\langle D_{ij}(\mathbf{q})D_{ij}(-\mathbf{q})\rangle$ is negative in transverse directions and positive along longitudinal directions, as shown in the Supplemental Material [13]. It is this property

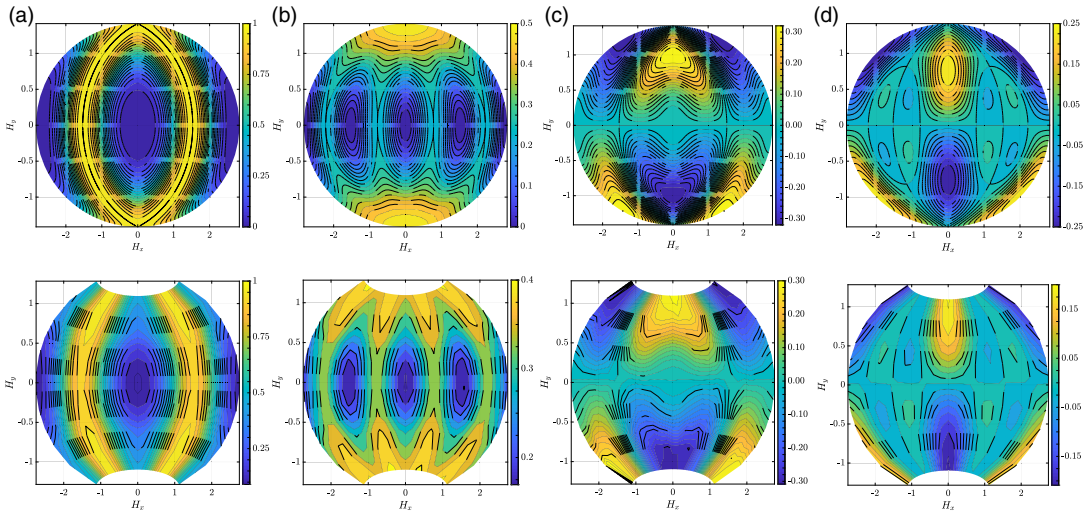

FIG. 2. Comparisons in Fourier space between theoretical predictions (top) and numerical results (bottom) from jammed packings of frictionless spheres in three dimensions. The figures display the radially averaged correlation functions (a) $C_{xxxx}(\theta,\phi)$, (b) $C_{xyxy}(\theta,\phi)$, (c) $C_{xxxz}(\theta,\phi)$ and (d) $C_{xyyz}(\theta,\phi)$, respectively. The coordinates (H_x, H_y) represent a Hammer projection of the (θ,ϕ) shell onto the plane. The results are presented for system size $N = 27000$, and have been averaged over 350 configurations. The range of packing fractions for these configurations is $\phi \in [0.686, 0.689]$ and the range of pressure per grain is $P \in [0.0136, 0.0147]$. Results for the $\hat{\Lambda}$ tensor have not been presented due to the small effective system size: $30 \times 30 \times 30$. The blank regions at the poles ϕ at $\theta = 0$ and $\theta = \pi$ in the numerical results is due to the difficulty in sampling these points.

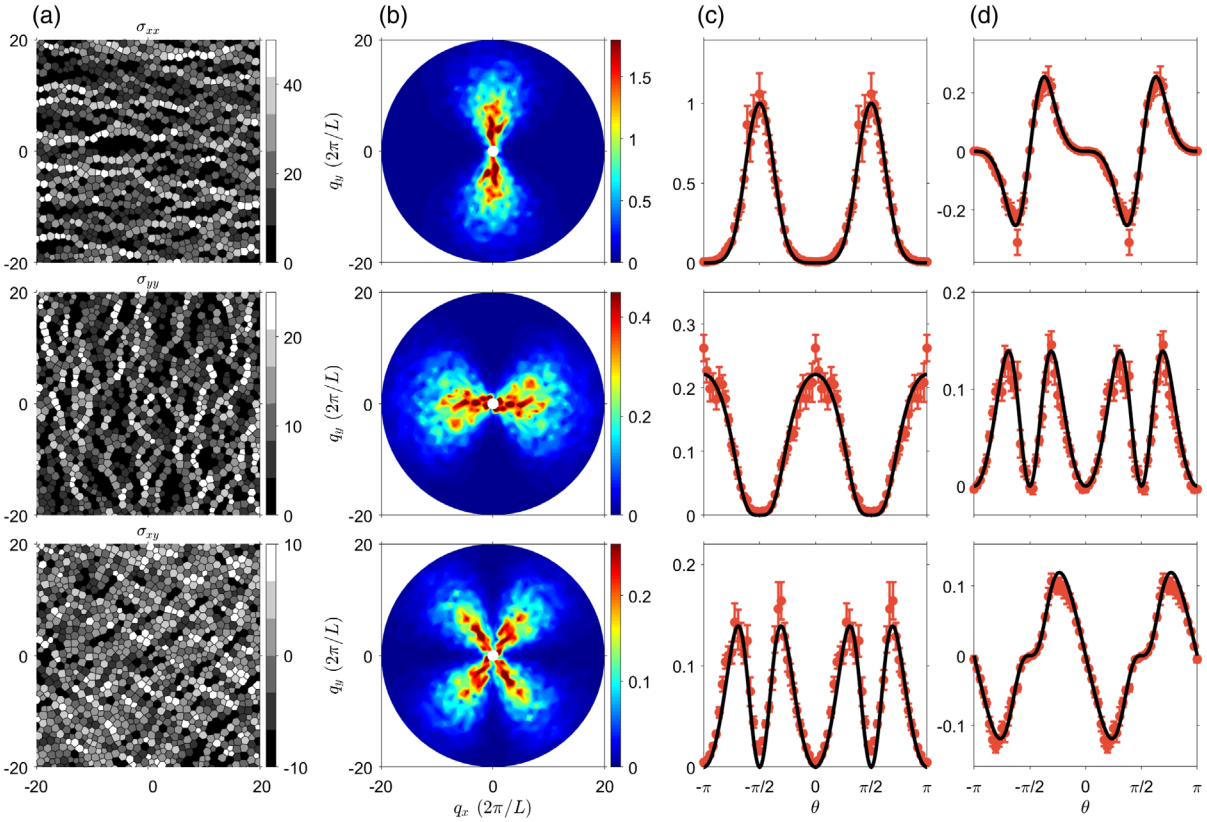

FIG. 3. Comparisons in Fourier space between the experimental results (red symbols) in *sheared* frictional packings and the theoretical predictions (black line). (a) Photoelastic images produced from a sheared packing. (b) Contour plots of the stress-stress correlation functions: $C_{xxxx}(q,\theta)$ (top), $C_{yyyy}(q,\theta)$ (middle) and $C_{xyxy}(q,\theta)$ (bottom). (c) Corresponding angular plots. (d) Angular plots of $C_{xxxy}(\theta)$ (top), $C_{xxyy}(\theta)$ (middle), and $C_{xyyy}(\theta)$ (bottom). All correlations are normalized by the peak value of $C_{xxxx}(\theta)$. The $\hat{\Lambda}$ tensor obtained from the fit is diagonal with $\lambda_{11} = 1$, $\lambda_{22} = 4.5$, and $\lambda_{33} = 1.46$. The ratio of the boundary stress components defining the shear is $\Sigma_{xx}/\Sigma_{yy} = 1.94$, which satisfies the positivity bound [37,39] $(\lambda_{22}/\lambda_{11}) \geq (\Sigma_{xx}/\Sigma_{yy})^2$.

that is strikingly demonstrated in photoelastic images of force chains in Fig. 3 and Figs. S2–S4 in the Supplemental Material [13].

Summary and outlook.—To summarize, we have demonstrated that the elasticity of athermal amorphous solids is described by an exact analog of the electrostatics of a fractonic $U(1)$ gauge theory [25] in polarizable media. Although our analysis focused on granular solids, it marks a paradigm shift in our understanding of amorphous elasticity for a much broader class of solids such as jammed suspensions [4], disordered crystals [40] and colloidal gels [6] with no broken symmetry but strictly enforced *local* constraints of force and torque balance. A key to the above approach is the lack of a *reference* configuration rendering $\boldsymbol{\phi}$ to be unobservable. In a crystal, this is no longer true. Further, the crystal can survive in a zero-stress condition. Based on these observations, our preliminary considerations suggest that the crystalline elasticity due to broken symmetry modifies the nature of the media, possibly involving a Higgs mechanism, i.e., a crystal is a momentum condensate [41]. In such a scenario, the plasmon excitations of the tensor electromagnetism would appear as optical phonons. However, the emergence of gapless acoustic phonons currently remains unclear.

The theory can be extended to stress correlations in thermal amorphous solids such as low-temperature glass formers [42–44]. As in frustrated magnets [8], thermal fluctuations lead to a length scale characterizing the distance between particles at which force and torque balance are violated, and wash out the pinch-point singularity [13]. This low-temperature extension does not include the physics of the glass transition, which addresses the onset of rigidity in supercooled liquids. The theory we have presented assumes that all disordered networks that satisfy the constraints of mechanical equilibrium are equiprobable. If and why the glass transition generates this ensemble is an important question that we have not addressed.

A fully dynamical theory of amorphous materials can be constructed by extending the "electrostatics" to "electrodynamics" through the identification of the analog of a magnetic field, and including unbalanced forces as charged excitations [26].

The authors acknowledge Michael D'Eon, Albion Lawrence, Debarghya Banerjee, Chandan Dasgupta, Kedar Damle, Roderich Moessner, Nandagopal M, Prasad Perlekar, Samriddhi Sankar Ray, and Vijay Shenoy for fruitful discussions. J. N. and B. C. acknowledge support from NSF-CBET-1916877 and BSF-2016188. B. C. was supported by a Simons Fellowship in Theoretical Physics. S. B. acknowledges financial support of Max Planck partner group on strongly correlated systems at ICTS; SERB-DST (Govt. of India) Early Career Research Grant (No. ECR/2017/000504) and the Department of Atomic Energy (DAE), Govt. of India, under Project No. 12-R&D-TFR-5.10-1100. Y. W. and J. Z. acknowledge the support from NSFC under (No. 11774221 and No. 11974238). B. C., J. N., and S. B. would like to thank the ICTS program: Entropy, Information and Order in SoftMatter (ICTS/EOISM2018/08) during which a part of the work was done. The work of J. N. and K. R. was funded in part by intramural funds at TIFR Hyderabad from the DAE.

[1] C. S. O'Hern, L. E. Silbert, A. J. Liu, and S. R. Nagel, Jamming at zero temperature and zero applied stress: The epitome of disorder, Phys. Rev. E **68**, 011306 (2003).
[2] D. Bi, J. Zhang, B. Chakraborty, and R. P. Behringer, Jamming by shear, Nature (London) **480**, 355 (2011).
[3] M. E. Cates, J. P. Wittmer, J.-P. Bouchaud, and P. Claudin, Jamming, Force Chains, and Fragile Matter, Phys. Rev. Lett. **81**, 1841 (1998).
[4] I. R. Peters, S. Majumdar, and H. M. Jaeger, Direct observation of dynamic shear jamming in dense suspensions, Nature (London) **532**, 214 (2016).
[5] M. E. Cates, M. Fuchs, K. Kroy, W. C. K. Poon, and A. M. Puertas, Theory and simulation of gelation, arrest and yielding in attracting colloids, J. Phys. Condens. Matter **16**, S4861 (2004).
[6] S. Zhang, L. Zhang, M. Bouzid, D. Zeb Rocklin, E. Del Gado, and X. Mao, Correlated Rigidity Percolation and Colloidal Gels, Phys. Rev. Lett. **123**, 058001 (2019).
[7] L. D. Landau, L. P. Pitaevskii, A. M. Kosevich, and E. Lifshitz, *Theory of Elasticity* (Elsevier, New York, 2012).
[8] H. Diep *et al.*, *Frustrated Spin Systems* (World Scientific, Singapore, 2013).
[9] D. A. Huse, W. Krauth, R. Moessner, and S. L. Sondhi, Coulomb and Liquid Dimer Models in Three Dimensions, Phys. Rev. Lett. **91**, 167004 (2003).
[10] C. Castelnovo, R. Moessner, and S. L. Sondhi, Magnetic monopoles in spin ice, Nature (London) **451**, 42 (2008).
[11] D. Bi, S. Henkes, K. E. Daniels, and B. Chakraborty, The statistical physics of athermal materials, Annu. Rev. Condens. Matter Phys. **6**, 63 (2015).
[12] E. DeGiuli, Continuum limits of granular systems, Ph.D. thesis, University of British Columbia, 2012.
[13] See Supplemental Material at http://link.aps.org/supplemental/10.1103/PhysRevLett.125.118002 for details, which includes Refs. [14–23].
[14] C. S. O'Hern, S. A. Langer, A. J. Liu, and S. R. Nagel, Random Packings of Frictionless Particles, Phys. Rev. Lett. **88**, 075507 (2002).
[15] K. Ramola and B. Chakraborty, Stress response of granular systems, J. Stat. Phys. **169**, 1 (2017).
[16] E. Bitzek, P. Koskinen, F. Gähler, M. Moseler, and P. Gumbsch, Structural Relaxation made Simple, Phys. Rev. Lett. **97**, 170201 (2006).
[17] J. Guénolé, W. G. Nöhring, A. Vaid, F. Houllé, Z. Xie, A. Prakash, and E. Bitzek, Assessment and optimization of the fast inertial relaxation engine (fire) for energy minimization in atomistic simulations and its implementation in LAMMPS, Comput. Mater. Sci. **175**, 109584 (2020).

[18] S. Plimpton, Fast parallel algorithms for short-range molecular dynamics, J. Comput. Phys. **117**, 1 (1995).
[19] Y. Wang, L. Hong, Y. Wang, W. Schirmacher, and J. Zhang, Disentangling boson peaks and van Hove singularities in a model glass, Phys. Rev. B **98**, 174207 (2018).
[20] E. DeGiuli and J. McElwaine, Laws of granular solids. Geometry and topology, Phys. Rev. E **84**, 041310 (2011).
[21] É. Lantagne-Hurtubise, S. Bhattacharjee, and R. Moessner, Electric field control of emergent electrodynamics in quantum spin ice, Phys. Rev. B **96**, 125145 (2017).
[22] C. Xu, Gapless bosonic excitation without symmetry breaking: An algebraic spin liquid with soft gravitons, Phys. Rev. B **74**, 224433 (2006).
[23] E. DeGiuli, Edwards field theory for glasses and granular matter, Phys. Rev. E **98**, 033001 (2018).
[24] R. C. Ball and R. Blumenfeld, Stress Field in Granular Systems: Loop Forces and Potential Formulation, Phys. Rev. Lett. **88**, 115505 (2002).
[25] M. Pretko, Generalized electromagnetism of subdimensional particles: A spin liquid story, Phys. Rev. B **96**, 035119 (2017).
[26] M. Pretko, The fracton gauge principle, Phys. Rev. B **98**, 115134 (2018).
[27] C. Domb, M. S. Green, and J. L. Lebowitz, *Phase Transitions and Critical Phenomena*, edited by C. Domb and J. Lebowitz (Academic Press, London, 1989), Vol. 13.
[28] N. W. Ashcroft and N. D. Mermin, *Solid State Physics* (Saunders College Publishing, Philadelphia, 1976).
[29] M. Pretko and L. Radzihovsky, Fracton-Elasticity Duality, Phys. Rev. Lett. **120**, 195301 (2018).
[30] T. S. Majmudar and R. P. Behringer, Contact force measurements and stress-induced anisotropy in granular materials, Nature (London) **435**, 1079 (2005).
[31] J.-P. Bouchaud, Granular media: Some ideas from statistical physics, in *Slow Relaxations and Nonequilibrium Dynamics in Condensed Matter*, edited by J. Bouchaud, J. L. Barrat, M. Feigelman, J. Kurchan, and J. Dalibard (EDP Sciences, Les Ulis, 2003), Vol. 77, pp. 185–202.
[32] M. Otto, J.-P. Bouchaud, P. Claudin, and J. E. S. Socolar, Anisotropy in granular media: Classical elasticity and directed-force chain network, Phys. Rev. E **67**, 031302 (2003).
[33] A. Lemaître, Stress correlations in glasses, J. Chem. Phys. **149**, 104107 (2018).
[34] J. Geng, D. Howell, E. Longhi, R. P. Behringer, G. Reydellet, L. Vanel, E. Clément, and S. Luding, Footprints in Sand: The Response of a Granular Material to Local Perturbations, Phys. Rev. Lett. **87**, 035506 (2001).
[35] C. Xu, Novel Algebraic boson liquid phase with soft Graviton excitations, arXiv:cond-mat/0602443.
[36] A. Prem, S. Vijay, Y. Z. Chou, M. Pretko, and R. M. Nandkishore, Pinch point singularities of tensor spin liquids, Phys. Rev. B **98**, 165140 (2018).
[37] S. Henkes and B. Chakraborty, Statistical mechanics framework for static granular matter, Phys. Rev. E **79**, 061301 (2009).
[38] E. DeGiuli, Field Theory for Amorphous Solids, Phys. Rev. Lett. **121**, 118001 (2018).
[39] G. Lois, J. Zhang, T. S. Majmudar, S. Henkes, B. Chakraborty, C. S. OHern, and R. P. Behringer, Stress correlations in granular materials: An entropic formulation, Phys. Rev. E **80**, 060303(R) (2009).
[40] P. Acharya, S. Sengupta, B. Chakraborty, and K. Ramola, Athermal Fluctuations in Disordered Crystals, Phys. Rev. Lett. **124**, 168004 (2020).
[41] P. Anderson, *Basic Notions Of Condensed Matter Physics* (CRC Press, Boca Raton, 1994).
[42] S. Gelin, H. Tanaka, and A. Lemaître, Anomalous phonon scattering and elastic correlations in amorphous solids, Nat. Mater. **15**, 1177 (2016).
[43] M. Maier, A. Zippelius, and M. Fuchs, Emergence of Long-Ranged Stress Correlations at the Liquid to Glass Transition, Phys. Rev. Lett. **119**, 265701 (2017).
[44] B. Wu, T. Iwashita, and T. Egami, Anisotropic stress correlations in two-dimensional liquids, Phys. Rev. E **91**, 032301 (2015).